Optimized Design of Multi-Speed Transmissions for Parallel Hybrid Electric Vehicles ⋆

Xuefang Li * **Boli Chen** ** **Simos A. Evangelou** ***

* *School of Intelligent Systems Engineering, Sun Yat-Sen University, Guangzhou 510275, China (e-mail: lixuef25@mail.sysu.edu.cn).*
** *Department of Electronic and Electrical Engineering, University College London, UK, (e-mail: boli.chen@ucl.ac.uk).*
*** *Department of Electrical and Electronic Engineering, Imperial College London, South Kensington Campus SW7 2AZ, UK (e-mail: s.evangelou@imperial.ac.uk)*

Abstract: In this paper, the optimal design of a multi-speed transmission system in terms of gear ratio, number of gears and gear shifting strategy is investigated for a parallel hybrid electric vehicle. The design procedure starts with the optimization of the transmission configuration to identify the optimal gear ratios for a specified number of gears. In order to avoid solving a complex co-optimization problem that involves numerous control variables for hybrid powertrain energy management (EM), gear ratios and gear shifting, the gear ratio optimization is properly decoupled from the co-optimization problem, while the optimal gear shifting strategy for the optimized gear ratios is determined jointly with the powertrain EM. The separation of the co-optimization makes it possible to solve individual problems by dynamic programming (DP), which guarantees global optimality. To show the impact of optimally designed and controlled transmission on fuel savings, the fuel economy solution of the proposed scheme is compared with the traditional EM and gear shifting optimization method that applies non-optimized gear ratios. Simulation examples verify the effectiveness of the proposed methodology and show the fuel savings incurred by the configuration optimization of the multi-speed transmission system.

1. INTRODUCTION

Due to the increase of CO2 levels and consumption of the finite supply of oil, the automotive industry is experiencing an inevitable paradigm shift from conventional powertrain to electrified powertrain. One of the viable solutions is the hybrid electric vehicle (HEV), which has been developed rapidly in the past two decades. HEVs as opposed to conventional vehicles are powered by multiple power sources, which enable extra dimensions in the powertrain control, as the power split between energy sources can be freely optimized in terms of fuel consumption and tailpipe emission. The problem of finding the proper power split for HEVs is referred to as energy management (EM) control problem, which has been investigated substantially in the literature (Sabri et al., 2016; Shabbir and Evangelou, 2016; Hou et al., 2014; Liu et al., 2017; Zeng and Wang, 2015; Kim et al., 2014; Chen et al., 2019).

Based on the arrangement of the hybrid powertrain components, hybrid electric powertrains can be categorized into series, parallel, and series-parallel topologies. In the case of the parallel architecture, the internal combustion engine (ICE) is mechanically connected to the wheels via a gearbox, and therefore, the operating points of the ICE do not only depend on the energy source power split but also depend on gearbox configuration and working pattern.In (Ngo et al., 2012), it has been shown that the optimally designed transmission system can further improve the performance of the EM strategies in terms of the fuel economy. However, most of EM strategies in the literature are developed for predetermined gearbox configurations and

gear shifting policies, which are usually non-optimal (Sabri et al., 2016; Li and Evangelou, 2019; Hou et al., 2014; Zeng and Wang, 2015). As such, these EM methods tend to yield suboptimal solutions.

Previous research has also considered the transmission optimization for parallel HEVs. For instance, a transmission-actuated EM strategy is proposed in (Sundstrom et al., 2009), where the equivalent consumption minimization strategy (ECM-S) is extended to offer the optimization solution of the gear shift strategy. In (Ngo et al., 2015), the energy losses of the gearbox are investigated for HEVs, where both EM and gear shift are jointly optimized. More recently, a distributed optimization approach is developed in (Joševski and Abel, 2016) aiming to solve the co-optimization problem of the EM and gear shifting control in two steps to reduced the computational complexity. The aforementioned works only focus on the gear shifting optimization. However, the optimization of the gear ratio and the number of gears, which are neglected, could alter the optimal gear shirting policy. Therefore, the present work investigates the optimization of all the mentioned aspects.

The investigation carried out in this paper is based on a typical parallel HEV with the through-the-road (TTR) powertrain architecture. Nevertheless, the ideas that are presented also have relevance to other parallel HEV architectures. The developed method is formed by two steps. First, an approach based on optimization and classification techniques is proposed to determine the number of gears and the corresponding gear ratios. Subsequently, a joint optimization of energy management and gear shifting is formulated and solved by dynamic programming (DP) (Sundstrom and Guzzella, 2009) to find the optimal

gear shifting strategy and power split for the optimized gearbox configuration obtained in the first step. The fuel economy solution of the proposed method is benchmarked against two approaches: a) a conventional EM method with fixed gear shifting policy and gear ratios, and b) the same two step optimization mechanism but with an idealized stepless gearbox, where the latter is expected to be better than the proposed method due the flexibility offered by the stepless gearbox. The comparative results show the effectiveness of the proposed method and fuel savings against the benchmark solution.

The rest of the paper is organized as follows. Section 2 introduces prelimimaries of the study, including the HEV powertrain model and test driving cycles. In Section 3, the gear ratio optimization approach is presented, while the joint optimization of energy management and gear shifting is described and tested in Section 4 by comparisons with the benchmark solutions. Finally, Section 5 draws the conclusions of this work.

2. PRELIMINARIES

2.1 Powertrain Architecture and Modelling

The TTR HEV powertrain used in this study is illustrated in Fig. 1. The powertrain includes an electric path and a fuel path, which drive two axles separately. The fuel path is formed
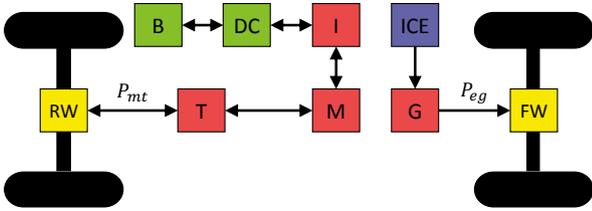

Fig. 1. Powertrain architecture of TTR HEV. B: battery, DC: D-C/DC converter, M: motor, I: DC/AC inverter, G: gearbox, T: fixed transmission; FW: front axle, RW: rear axle.

by an ICE that converts chemical fuel power to mechanical propulsion power. The ICE is connected to the front axle through a stepped transmission. On the other hand, the electric branch is powered by the battery that provides the power to the electric machine to drive the rear axle when the electric machine is motoring, and the battery can regenerate kinetic energy by turning the electric machine into a generator during braking.

According to the vehicle longitudinal dynamics, the total driving power demand P_{pl} requested to follow a given driving cycle can be evaluated by

$$P_{pl} = (m\frac{dv}{dt} + f_T mg + f_D v^2)v \qquad (1)$$

where m is the vehicle mass, v is the vehicle speed, f_T is the rolling resistance coefficient and f_D is the aerodynamics drag coefficient. The requested driving power is met by the power outputs of both branches and the possible mechanical braking power, expressed as

$$P_{pl} = P_{mt} + P_{eg} + P_h \qquad (2)$$

where P_{mt} and P_{eg} represent the final driving power delivered by the electric and ICE branches, respectively, and P_h denotes the mechanical braking power directly applied to the wheels. The electric branch allows the regenerative braking that conveys braking power (negative P_{pl}) up to the battery. In the present

work, it is assumed that the power regeneration is only restricted by the battery charging power limit, and when the limit is reached, mechanical brakes are actuated to provide the rest of the braking power.

The detailed powertrain model has been presented in previous work (Li and Evangelou, 2019), where the ICE and electric motor are modeled by steady state efficiency maps with respect to the toque and angular speed, while other powertrain components are simply modeled by constant efficiency factors. For the sake of brevity, let us define the efficiencies of electric and fuel paths respectively by $\eta_{mt}(T_{lm}, \omega_m) = \eta_{dc}\eta_t\eta_i\eta_m(T_{lm}, \omega_m)$ and $\eta_{eg}(T_e, \omega_e) = \eta_g\eta_e(T_e, \omega_e)$, where $\eta_e, \eta_m, \eta_g, \eta_{dc}, \eta_i, \eta_t$ are the efficiencies of the ICE, motor, gearbox, DC/DC converter, DC/AC inverter and fixed gear transmission, respectively, T_e is the ICE torque, ω_e is the ICE speed, and T_{lm} and ω_m are the torque and speed of the electric motor respectively. The overall powertrain system dynamics are given by

$$\frac{d}{dt}\begin{pmatrix} m_f \\ \text{SOC} \end{pmatrix} = \begin{pmatrix} \dfrac{P_{eg}}{\eta_{eg}(T_e, \omega_e)Q_{LHV}} \\ -\dfrac{P_{mt}}{(\eta_{mt}(T_{lm}, \omega_m))^{\text{sign}(P_{mt})}V_bQ_{\max}} \end{pmatrix} \qquad (3)$$

where m_f represents the fuel mass, SOC denotes the battery state-of-charge, Q_{LHV} is the gasoline lower heating value, V_b is the battery voltage, determined by

$$V_b = V_{oc} - i_b R_b$$

with V_{oc} the battery open circuit voltage, R_b the battery internal resistance and i_b the battery current assumed positive during the discharge phase. The engine speed ω_e is coupled with the vehicle speed via the stepped gearbox, as follows:

$$\omega_e = \frac{g_{e,i}g_{fd}}{r_{wheel}}v \qquad (4)$$

where $g_{e,i}$ represents the ith gear ratio, g_{fd} is the final drive ratio, and r_{wheel} is the wheel radius. The HEV powertrain parameters are listed in Table 1.

Table 1. Main Vehicle Model Parameters

symbol	value	description
m	1770 kg	vehicle mass
f_T	0.01	rolling resistance coefficient
f_D	0.47	aerodynamics drag coefficient
r	0.305m	Wheel radius
g_m	2.9	motor transmission ratio
$Q_{\max}$	5.65 Ah	battery capacity
R_b	0.2056 Ω	battery internal resistance
V_{oc}	230 V	battery open circuit voltage
$P_{b,\min/b,\max}$	$27/-15$kW	max/min battery power
η_i	0.96	efficiency of inverter
η_{dc}	0.96	efficiency of converter
η_t	0.96	efficiency of motor transmission
η_g	0.96	efficiency of the gearbox
$P_{e,\max}$	120kW	maximum ICE power
$T_{e,\max}$	300Nm	maximum ICE torque
$P_{m,\min/m,\max}$	$27/-27$kW	max/min motor power
$T_{m,\min/m,\max}$	$200/-200$Nm	max/min motor torque

2.2 Driving cycles

In this work, the co-optimization problem of energy management and gearbox ratios as well as gear shifting strategy are investigated by numerical optimization in which the vehicle follows defined speed profiles according to specific driving cycles. The WLTP (worldwide harmonized light vehicles test

procedure) corresponds to the latest test procedure adopted by industry and it is therefore utilized in the present work. As shown in Fig. 2, the WLTP profile is a single driving cycle with four stages, defined by their speed: low (WL-L), medium (WL-M), high (WL-H) and extra high (WL-E). Each of the stages can be considered on their own as independent driving cycles.
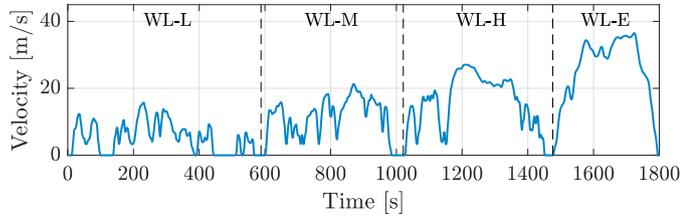

Fig. 2. Speed profile of the WLTP with four different stages according to the average speed.

3. GEAR RATIO OPTIMIZATION

This section presents a method to identify the optimal gear ratios of the stepped transmission. To isolate the gear ratio optimization from the gear shift and EM optimization problems, let us first neglect the electric path by considering a conventional powertrain with only the fuel path as shown in Fig. 1.

3.1 Gear ratio optimization

In view of (3), the system dynamics of a conventional powertrain can be expressed as

$$\frac{d}{dt} m_f = \frac{P_{eg}}{\eta_{eg}\left(T_e, \frac{g_{e,i} g_{fd} v}{r_{wheel}}\right) Q_{LHV}} \tag{5}$$

where $P_{eg} = \max(0, P_{pl})$ as $P_{eg} \geq 0$, whereas the negative power is met by mechanical brakes. As such, the gear ratio $g_{e,i}$ now becomes the only control variable. Since both the number of gears and the gear ratios are unknown, we initially assume the gearbox is stepless, such that the gear ratio is enabled to achieve any value within the permissible set $[g_{e,\min}, g_{e,\max}]$. In this work, the maximum and minimum gear ratios are set to 3.54 and 0.53, respectively (Li and Evangelou, 2019).

To determine the optimal gear ratios, the following optimal control problem (OCP) is formulated

$$\min_{g_{e,i}} \quad m_f(t_f) \tag{6a}$$

$$\text{subject to :} \quad \frac{d}{dt} m_f = \frac{P_{eg}}{\eta_{eg}\left(T_e, \frac{g_{e,i} g_{fd} v}{r_{wheel}}\right) Q_{LHV}} \tag{6b}$$

$$0 \leq P_{eg} \leq P_{eg,\max} \tag{6c}$$

$$g_{e,\min} \leq g_{e,i} \leq g_{e,\max} \tag{6d}$$

where the objective is to minimize the fuel consumption at the end of the mission with t_f the duration of the mission and $P_{eg,\max} = \eta_g P_{e,max}$. The OCP (6) is solved by DP for the four stages of the WLTP cycle, respectively. To emulate the continuous variable transmission system, the control variable $g_{e,i}$ is uniformly gridded within $[g_{e,\min}, g_{e,\max}]$ with a sufficiently large number N:

$$U_g = \left\{ g_{e,i} : g_{e,i} = g_{e,\min} + \frac{i-1}{N} (g_{e,\max} - g_{e,\min}), i = 1, \dots, N \right\} \tag{7}$$

where the set U_g includes all possible gear ratio values for a given N. For illustration purpose, the optimal trajectories of the gear ratio with $N = 1000$ for WL-M and WL-E are shown in Fig. 3.
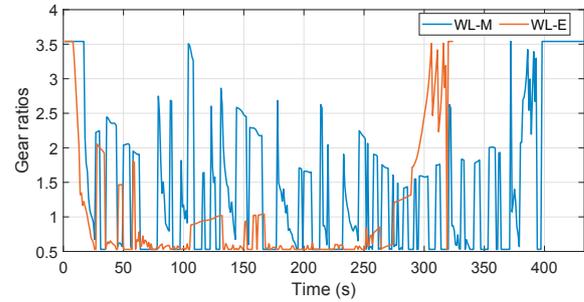

Fig. 3. Variations of the optimal gear ratio when driving WL-M and WL-E.

3.2 Data clustering

By collecting the optimal gear ratios solved for all four WLTP driving cycles, the next step is to cluster the data to determine the stepped gear ratios for specified numbers of gears. In the present work, k-means clustering method is applied to classify the collected data (Lloyd, 1982). Given a data set $(\mathbf{x}_1, \mathbf{x}_2, \dots, \mathbf{x}_n)$ with $\mathbf{x}_i \in \mathbb{R}^d$, the k-means clustering method partitions the given data set into $k(\leq n)$ sets $S = \{S_1, S_2, \dots, S_k\}$ so as to minimize

$$\arg\min_S \sum_{j=1}^{k} \sum_{\mathbf{x} \in S_j} \|\mathbf{x} - \mu_j\|$$

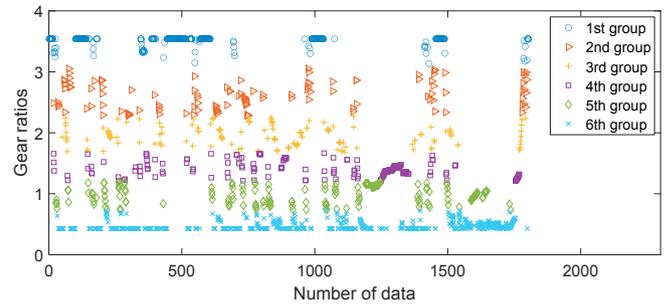where μ_j is the mean of points in S_j.

Fig. 4. Clustering of gear ratios by k-means.

For illustration purposes, Fig. 4 shows the clustering result for a 6-speed transmission, and the corresponding gear ratios are the mean values of each group, which are presented in Table 2. Similarly, the gear ratios for 4-, 8- and 10-speed transmissions can be calculated (In the present work, we just consider even number of gears for illustration purpose). The results are also summarized in Table 2. In order to determine the number of gears, the discretized gear ratios in Table 2 will be applied to the parallel HEV model, which will be specified in the next section.

4. JOINT ENERGY MANAGEMENT AND GEAR SHIFTING OPTIMIZATION

In parallel HEVs, in addition to the gearbox configuration, the gear shifting policy, that determines the gear ratios at each time instance, will also affect the operating points of the powertrain, and thus the fuel economy. To explore the impact of gear

Table 2. Optimized gear ratios for different transmission systems

	4-speed	6-speed	8-speed	10-speed
1st gear ratio	3.4892	3.5138	3.5160	3.5330
2nd gear ratio	2.2407	2.6317	2.8151	3.1856
3rd gear ratio	1.3032	1.9850	2.3843	2.6459
4th gear ratio	0.4924	1.4129	2.0145	2.1754
5th gear ratio		0.9942	1.7001	1.8060
6th gear ratio		0.4659	1.3168	1.4101
7th gear ratio			0.9342	1.1369
8th gear ratio			0.4645	0.8634
9th gear ratio				0.5719
10th gear ratio				0.4376

shifting optimization on fuel savings, this section aims at joint optimization of energy management and gear shifting.

4.1 Gear shifting dynamics

The gear position dynamics is expressed by the following discrete equation

$$n_g(k+1) = n_g(k) + u_g(k), \; k \in \mathbb{Z}^+ \qquad (8)$$

with $n_g(k)$ being the gear position and satisfying $n_g(k) \in [1, N_g]$ with $N_g > 1$ being the number of gears. In the present work, for the reason of acceptable driveability, the gearshift control variable is set as $u_g(k) \in \{-1, 0, 1\}$ to avoid dramatic changes in engine speed.

4.2 Joint optimization formulation

Given a predefined driving cycle with the time length t_f, the objective of the optimization is to find an optimal control law $\mathbf{u}^* = [P_{eg}^*, P_{mt}^*, u_g^*]$ such that the fuel consumption over the entire driving cycle is minimized. The optimization problem is formulated as follows

$$\min_{\mathbf{u}} \; m_f(t_f) \qquad (9a)$$

$$\text{subject to}: \; \dot{\mathbf{x}} = \mathbf{f}(\mathbf{x}, \mathbf{u}), \qquad (9b)$$

$$n_g(k+1) = n_g(k) + u_g(k), \qquad (9c)$$

$$P_{pl} = P_{eg} + P_{mt} + P_h, \qquad (9d)$$

$$0 \le P_{eg} \le P_{eg,\max}, \qquad (9e)$$

$$P_{mt,\min} \le P_{mt} \le P_{mt,\max}, \qquad (9f)$$

$$SOC_{\min} \le SOC \le SOC_{\max}, \qquad (9g)$$

$$SOC(0) = 0.65, \; SOC(t_f) = SOC(0), \qquad (9h)$$

where the dynamic model (9b) has already been specified in (3) with $\mathbf{x} = [m_f, SOC]$. k in (9c) represents the sampling time being set to 1 in simulations. $P_{mt,\min}$ and $P_{mt,\max}$ represent the minimum and maximum power of the battery branch at the transmission, respectively, and the two limit values can be calculated from $P_{b,\min}$ and $P_{b,\max}$ (see Table 1) through the equation

$$P_b = (\eta_{dc} \eta_i \eta_m (T_m, \omega_m) \eta_t)^{\text{sign}(-P_{mt})} P_{mt}.$$

The maximum and minimum battery state of charge $SOC_{\max}$, $SOC_{\min}$ are set to 0.8 and 0.5, respectively.

It is well-known that DP is able to provide the global optimum solution to optimization problems. The present work will implement the DP algorithm developed in (Sundstrom and Guzzella, 2009). As the DP solves a discrete-time optimal control problem, the engine fuel consumption dynamics (fuel mass rate) can be considered into the cost function. Therefore, for the above optimal control problem (9), there are only two

dynamical constraints. One is the SOC as given in the second equation in (3), and another is the dynamics of gear shifting. In the DP algorithm, the dynamics of SOC is discretized based on the Euler method with a sampling period of 0.1 s. Furthermore, the grid points for the state and input variables are set to 501 which is reasonably large to ensure the accuracy of the simulation results.

4.3 Numerical results

In this section, the joint optimization problem expressed in (9) is solved with different gearbox configurations, which shows the impact of the optimally designed and controlled transmission on fuel savings of parallel HEVs in addition to energy management.

First of all, the impact of the number of gears to fuel consumption will be investigated. For the purpose of comparison, five scenarios with 4, 6, 8, 10 gears and a continuous gear shifting case are implemented to the parallel HEV model presented in Section 2. For the first four cases, the optimized gear ratios are applied, which have already been presented in Table 2 and the gear shifting dynamics has been given in (8). For the continuous gear shifting case, we allow the gear ratio to vary freely in the interval $[0.53, 3.54]$. The simulation results are presented in Table 3. For easy comparison, the results are plotted in Fig. 5. It is obvious that the more the gears, the better the performance in terms of fuel economy. In practice, however, adding more gears increases both the manufacturing and packaging cost. It is thought that the 6-speed gearbox is sufficient to the considered parallel HEV model with the corresponding gear ratios provided in Table 2.

Table 3. Comparison of fuel consumptions for joint optimization with different gearbox configurations

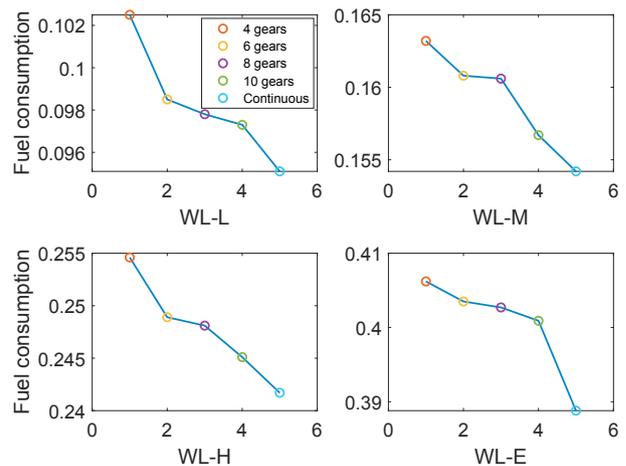| Driving cycles	4-speed	6-speed	8-speed	10-speed	continuous
WL-L	0.1025	0.0985	0.0978	0.0973	0.0951
WL-M	0.1632	0.1608	0.1606	0.1567	0.1542
WL-H	0.2546	0.2489	0.2481	0.2451	0.2417
WL-E	0.4062	0.4035	0.4027	0.4009	0.3888

Fig. 5. Fuel consumption obtained by the optimization with different gearbox configurations when driving WL-L, WL-M, WL-H and WL-E. The horizontal axis in each plot represents the number of gearbox configurations we considered.

Secondly, to show the potential fuel saving incurred by gear shifting optimization, we assume the TTR HEV is equiped with a 6-speed transmission. In contrast to the above joint optimization results, a benchmark scenario (power-split-only optimization) is conducted to optimize the power split only with a fixed gearbox configuration and shifting policy. In this case, the fixed gear shifting strategy is presented in Fig. 6 with the gear ratios given in Table 4, which has been applied in (Li and Evangelou, 2019).
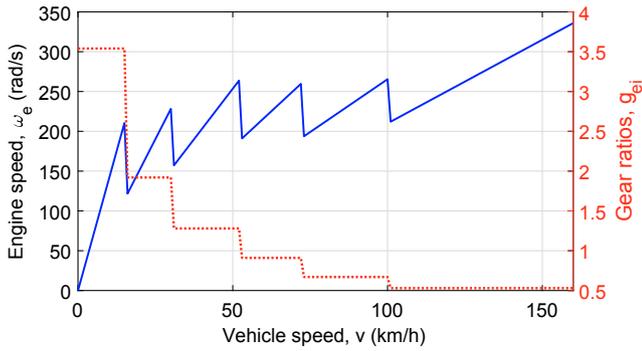

Fig. 6. Gear ratios and relationship between vehicle speed and engine speed.

Table 4. Gear ratio values

	Gear ratio
1st gear ratio	3.54
2nd gear ratio	1.92
3rd gear ratio	1.28
4th gear ratio	0.91
5th gear ratio	0.67
6th gear ratio	0.53
Final drive ratio	4.35

The simulation results are presented and compared in Table 5, where 'Joint-6-speed' represents the joint optimization with 6 optimized gear ratios obtained in Section 3 and 'Joint-continuous' represents the joint optimization with gear ratio varying freely in the interval [0.53, 3.54]. The improvement in terms of fuel consumption with different driving cycles are shown in Fig. 7, where it can be seen that with gear shifting optimization, the final fuel consumption can be reduced by 1.83% − 6.01% by optimizing the gear shifting together with energy management, with a combined difference (considering the four driving cycles together) of 3.64%, in comparison to the power-split-only optimization. Furthermore, we can see that the joint optimization with the stepless gearbox outperforms the power-split-only optimization by 5.54%-9.26%, with a combined difference of 7.01%, which implies that the fuel efficiency of parallel HEVs would be improved further significantly if the number of gears, gear ratios and shifting strategy can be optimized in a systematic way.

Table 5. Comparison of fuel consumptions with different gearbox configurations

Driving cycles	Power-split-only	Joint-6-speed	Joint-continuous
WL-L	0.1048	0.0985	0.0951
WL-M	0.1683	0.1608	0.1542
WL-H	0.2614	0.2489	0.2417
WL-E	0.4116	0.4035	0.3888

Furthermore, the variations of gear ratio for both the power-split-only and joint optimization with 6-speed transmission when driving WL-L, WL-M, WL-H and WL-E are presented
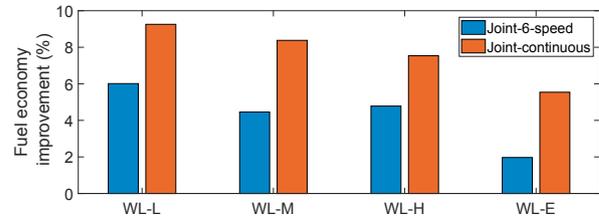

Fig. 7. Comparison of fuel consumption for joint optimization relative to the power-split-only optimization when driving the WL-L, WL-M, WL-H and WL-E.
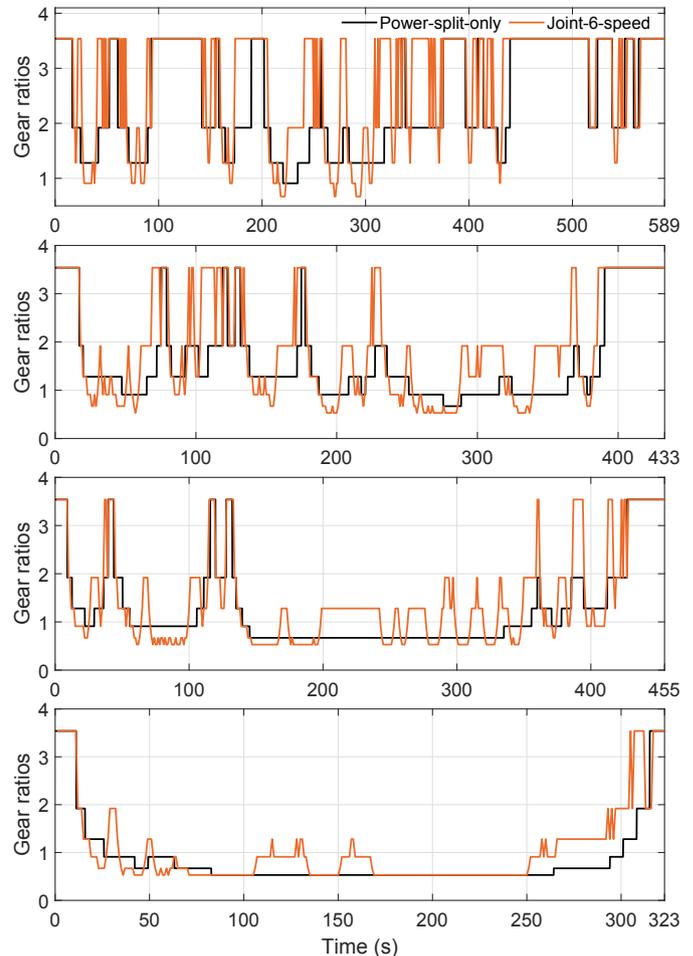

Fig. 8. The comparison of gear ratio variations for the power-split-only optimization and the joint optimization of energy management and gear shifting with a 6-speed transmission when driving WL-L, WL-M, WL-H and WL-E (top to bottom).

in Fig. 8, from which we can see that the operation of two different gearbox configurations are quite different. Due to direct connection of the ICE and the gearbox, the operating points of the ICE are surely affected by the gear ratios, as shown in Fig. 9. It is obvious that with the optimized gear ratios and shifting, the efficiency of the ICE is improved significantly, as the operating points with efficiency below 0.25 are almost avoided.

In addition to the engine efficiency, the variation of SOC profiles for both the joint optimization and power-split-only optimization are also presented in Fig. 10. It is obvious that with the joint optimization, the SOC profiles are more steady than the power-split-only optimization for WL-L, WL-M, WL-H, which
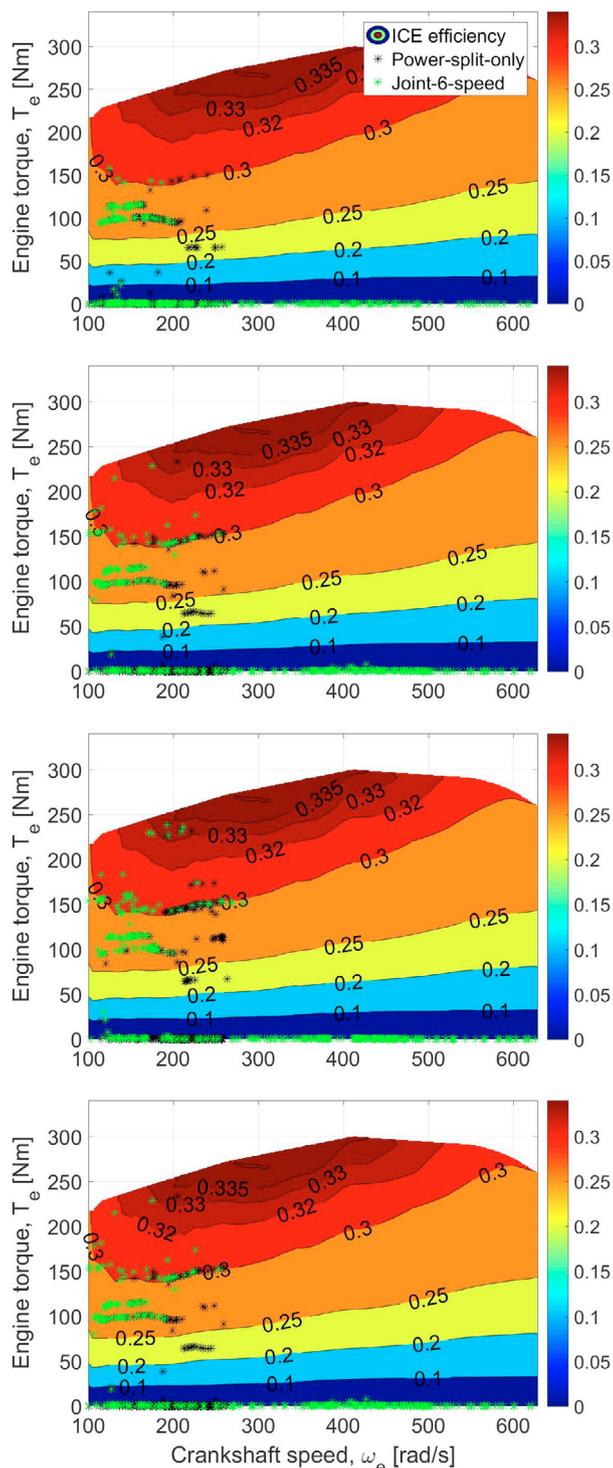
Fig. 9. The operating points of ICE for different optimization cases when driving WL-L, WL-M, WL-H and WL-E (top to bottom).
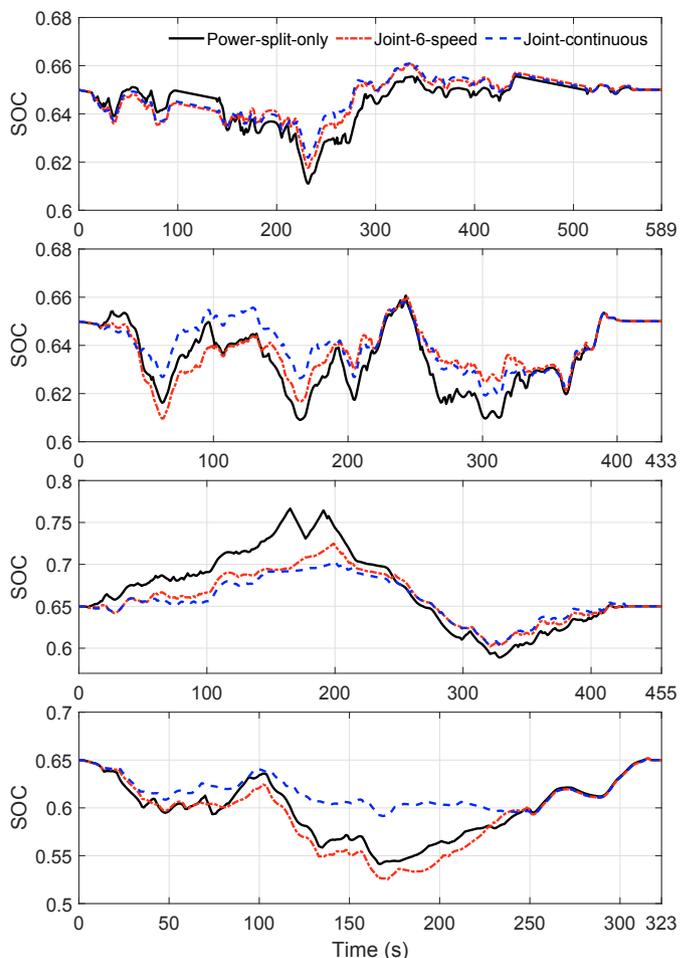

Fig. 10. SOC profiles of different optimization cases for the driving cycles WL-L, WL-M, WL-H and WL-E (top to bottom).

mization of parallel HEVs need to be conducted in future work by taking the hybrid powertrain into account.

5. CONCLUSION

In the present work, we investigate the optimal design of a multi-speed transmission system in terms of gear ratio, number of gears and gear shifting strategy for parallel hybrid electric vehicles (HEVs). In order to reduce the computational complexity, the gear ratio optimization is conducted firstly by being properly decoupled from the joint optimization problem of hybrid powertrain energy management (EM), gear ratios and gear shifting, after which the optimal gear shifting strategy with the optimized gear ratios is determined jointly with the powertrain EM. To show the impact of optimally designed and controlled transmission on fuel savings, the fuel economy solution of the proposed scheme is compared with the traditional EM and gear shifting optimization method that applies non-optimized gear ratios. Numerical results verify the effectiveness of the proposed methodology and demonstrate that the gearbox configuration optimization of the multi-speed transmission will improve the fuel economy of parallel HEVs significantly. In the next research phase, further investigations to develop an approach to optimize the gear ratios by taking the powertrain characteristics into account would be conducted. Moreover, it is worthwhile to design an optimized gear shift strategy for parallel HEVs that can be implemented in real-time.

is influenced by the efficiency characteristics of the battery branch. For WL-E, the SOC variation of the joint optimization with 6-speed transmission is even bigger than that of power-split-only optimization, and the difference between joint optimization with 6-speed transmission and stepless gearbox is also apparent, which implies that the current gear ratio optimization approach may not be good enough for all driving cycles, such as WL-E. Therefore, further investigations on gear ratio opti-

REFERENCES

Chen, B., Evangelou, S., and Lot, R. (2019). Series hybrid electric vehicle simultaneous energy management and driving speed optimization. *IEEE/ASME Transactions on Mechatronics*, 24(6), 2756–2767.

Hou, C., Ouyang, M., Xu, L., and Wang, H. (2014). Approximate pontryagins minimum principle applied to the energy management of plug-in hybrid electric vehicles. *Applied Energy*, 115, 174–189.

Joševski, M. and Abel, D. (2016). Gear shifting and engine on/off optimal control in hybrid electric vehicles using partial outer convexification. In *2016 IEEE Conference on Control Applications (CCA)*, 562–568. IEEE.

Kim, M., Jung, D., and Min, K. (2014). Hybrid thermostat strategy for enhancing fuel economy of series hybrid intracity bus. *IEEE Transactions on Vehicular Technology*, 63(8), 3569–3579.

Li, X. and Evangelou, S.A. (2019). Torque-leveling threshold-changing rule-based control for parallel hybrid electric vehicles. *IEEE Transactions on Vehicular Technology*, 68(7), 6509–6523.

Liu, T., Hu, X., Li, S.E., and Cao, D. (2017). Reinforcement learning optimized look-ahead energy management of a parallel hybrid electric vehicle. *IEEE/ASME Transactions on Mechatronics*, 22(4), 1497–1507.

Lloyd, S. (1982). Least squares quantization in pcm. *IEEE Transactions on Information Theory*, 28(2), 129–137.

Ngo, V., Hofman, T., Steinbuch, M., and Serrarens, A. (2015). Effect of gear shift and engine start losses on energy management strategies for hybrid electric vehicles. *International Journal of Powertrains*, 4(2), 141–162.

Ngo, V., Hofman, T., Steinbuch, M., and Serrarens, A. (2012). Optimal control of the gearshift command for hybrid electric vehicles. *IEEE Transactions on Vehicular Technology*, 61(8), 3531–3543.

Sabri, M., Danapalasingam, K., and Rahmat, M. (2016). A review on hybrid electric vehicles architecture and energy management strategies. *Renewable and Sustainable Energy Reviews*, 53, 1433–1442.

Shabbir, W. and Evangelou, S.A. (2016). Exclusive operation strategy for the supervisory control of series hybrid electric vehicles. *IEEE Transactions on Control Systems Technology*, 24(6), 2190–2198.

Sundstrom, O. and Guzzella, L. (2009). A generic dynamic programming matlab function. In *IEEE Control Applications,(CCA) & Intelligent Control (ISIC)*, 1625–1630.

Sundstrom, O., Soltic, P., and Guzzella, L. (2009). A transmission-actuated energy-management strategy. *IEEE Transactions on Vehicular Technology*, 59(1), 84–92.

Zeng, X. and Wang, J. (2015). A parallel hybrid electric vehicle energy management strategy using stochastic model predictive control with road grade preview. *IEEE Transactions on Control Systems Technology*, 23(6), 2416–2423.